Journal of Environmental Chemical Engineering 12 (2024) 111782

Contents lists available at ScienceDirect

Journal of Environmental Chemical Engineering

journal homepage: www.elsevier.com/locate/jece

Enhancing energy efficiency and H_2 production in lab-scale dual chamber microbial electrolysis cells: A focus on catholyte composition and voltage losses

Lorenzo Cristiani [a,*,1], Marco Zeppilli [a,*], Damiano Feriaud [a], Clara Marandola [a], Marco Petrangeli Papini [a], Serge Da Silva [b], Benjamin Erable [c], Marianna Villano [a]

[a] Department of Chemistry, Sapienza University of Rome, P.Le Aldo Moro 5, 00185 Rome, Italy
[b] 6T-MIC Ingénieries, 9 rue du développement – ZI de Vic, 31320 Castanet-Tolosan, France
[c] Laboratoire de Génie Chimique, Université de Toulouse, CNRS, INPT, UPS, Toulouse, France

ARTICLE INFO

Keywords:
Hydrogen production
Microbial electrolysis cell
Wastewater treatment
Buffer solution

ABSTRACT

Microbial electrolysis cells (MECs) have emerged as a promising technology for sustainable hydrogen production from wastewater treatment. An MEC consists of a microbial anode and a hydrogen evolution cathode, where microorganisms in the anode oxidize organic compounds, allowing the cathodic hydrogen production at lower potentials compared to abiotic electrolysis. The present study focuses on optimizing the catholyte composition and configuration in a MEC reactor to maximize hydrogen production rates while minimizing energy consumption. Indeed, buffer solutions of HCO_3^-, HPO_4^{2-}, and $H_2PO_4^-$ at different concentrations and operation mode were tested as catholytes analysing hydrogen production rates and energy consumptions of the process. The results demonstrate the stability of the anodic electroactive biofilm over a 220-day period, achieving consistent COD removal and hydrogen production. The findings reveal that the catholyte composition and operating mode significantly affect the cathodic performances of the MEC. Indeed, catholytes with higher buffer concentrations allow for a limited catholyte alkalinisation improving hydrogen production rates while a low buffer solution promotes an increase in process energy consumption. Bicarbonate buffer solution utilized under batch operation mode showed the better performances for hydrogen production at the cathodic side of MECs showing a higher cathodic coulombic efficiency coupled with stable pH levels and cathodic potentials. Overall, this research demonstrates the potential of MECs for sustainable hydrogen production and highlights the importance of optimizing catholyte composition and operating mode to increase energy efficiency of process.

1. Introduction

In order to comply with the goals set during the 2015 Paris climate agreement and avoid raising the global temperature above 2 °C, within 2050 humanity will have to reduce 80% of its greenhouse gas (GHG) emissions [1]. The sectors that produce the highest amount of GHG are energy production, heating, transport, industry, and agriculture. Green hydrogen is considered a sustainable fuel because its combustion produces exclusively water and no other side-products, although to guarantee that the hydrogen used has no release of GHG it must be produced from non-fossil resources. Nowadays 96% of the hydrogen is still produced from coal, petroleum or natural gas through steam reforming process [2,3], hydrogen is mainly used as a chemical to produce ammonia and automotive gasoline. This is the cheapest and most used process for hydrogen production nowadays and it has a thermal efficiency of 75–80% and it emits 7–10 gCO_2/gH_2. Among different technologies for sustainable hydrogen production under investigation, alkaline electrolyser results the most promising one, especially when

List of abbreviations: MEC, microbial electrolysis cell; COD, chemical oxygen demand; CE, coulombic efficiency; EC_{COD}, energy consumption for COD removal; rH_2, hydrogen production rate; CCE, cathodic coulombic efficiency; EC_{H2}, energy consumption for hydrogen production.

* Corresponding authors.
E-mail addresses: Lorenzo.cristiani@leibniz-hki.de (L. Cristiani), marco.zeppilli@uniroma1.it (M. Zeppilli).
[1] Current address: Department of Bio Pilot Plant, Leibniz Institute for Natural Product Research and Infection Biology - Hans-Knöll Institute, Adolf-Reichwein-Str. 23 07745 Jena, Germany

https://doi.org/10.1016/j.jece.2023.111782
Received 4 July 2023; Received in revised form 2 November 2023; Accepted 19 December 2023
Available online 21 December 2023

renewable electricity is used for the running of the process [3,4]. Alkaline electrolyzers work at a current density of 100–300 mA/cm^2 and have an energy efficiency of 50–60% [5]. Unlike steam methane reforming (SMR), electrolysis has the advantage of producing much purer hydrogen [6]. Producing H_2 through water electrolysis requires theoretically an electromotive force of + 1.23 V, an interesting approach could be the utilization of another anodic reaction for decreasing the theoretical electromotive force of the process. A promising technology, known as microbial electrolysis cells (MECs), was first proposed in 2005 [7–9]. The core of an MEC consists of a microbial anode and an "almost conventional" hydrogen evolution cathode. Some microorganisms spontaneously colonize the anode surface and form an electroactive biofilm, which acts as the electro-catalyst [10–12]. Thanks to this biofilm, the microbial anode can oxidize a large variety of low-cost carbon compounds [13–15]. The main advantage of MEC versus abiotic water electrolysis is the replacement of water oxidation by the oxidation of organic compounds, which can occur at significantly lower redox potentials with a significant reduction of energy [16–20]. The thermodynamic cell voltage of an MEC is thus considerably reduced with respect to the + 1.23 V threshold of water electrolysis in standard conditions, indeed, considering the oxidation of a single substrate like acetate, the electromotive force of the cell results in + 0.187 V, an 85% lower value [9,21,22]. Another advantage of MECs is the fact that their substrate can be wastewaters, which are currently treated with the activated sludge process which has an energetic cost of 1.2 kWh/kgCOD [23], for this reason MECs have been promoted as an emerging technology that could improve the energy balance of wastewater treatment by coupling it with fuel production [24,25]. It's worth noting that in the last two decades, scientists tried to optimize the process to reduce energy consumption and enhance its attractiveness. Numerous strategies have been adopted to diminish internal resistance. However, when scaling up the process, more careful consideration should be given to other factors, such as material stability, membrane fouling, electrode passivation, and overall cell design, to ensure the optimal performance and longevity of the microbial electrolysis cell. In this study, a two-compartment 1.7 L MEC reactor was operated continuously, with a synthetic wastewater fed to the anodic chamber for over 220 days with the main to establish a continuous production of hydrogen with minimal energy costs. Specifically, the aims were to achieve a constant anodic current generation while maintaining a stable anode overpotential and reducing the cathode overvoltage to a minimum in the long term. Modifications were made to the catholyte composition and cathodic fluid dynamics, and the performance and energy assessment were evaluated, taking into account every aspect of the processes. The cathodic compartment was operated in both batch and continuous flow mode using different catholytes: diluted and concentrated solutions of HCO_3^-, HPO_4^{2-}, and $H_2PO_4^-$. These catholytes were selected based on previous studies [23,26] that demonstrated the potential of weak mineral acids to catalyse the hydrogen evolution reaction. This study aims to investigate MEC performance for H_2 production while, in the course of a long-term experiment, assessing the possibility to develop a resilient biobased process.

2. Materials and methods

2.1. Microbial electrolysis cell

The MEC used in this study consisted of two identical Plexiglass frames, with internal dimensions of 17 cm × 17 cm× 3 cm, bolted

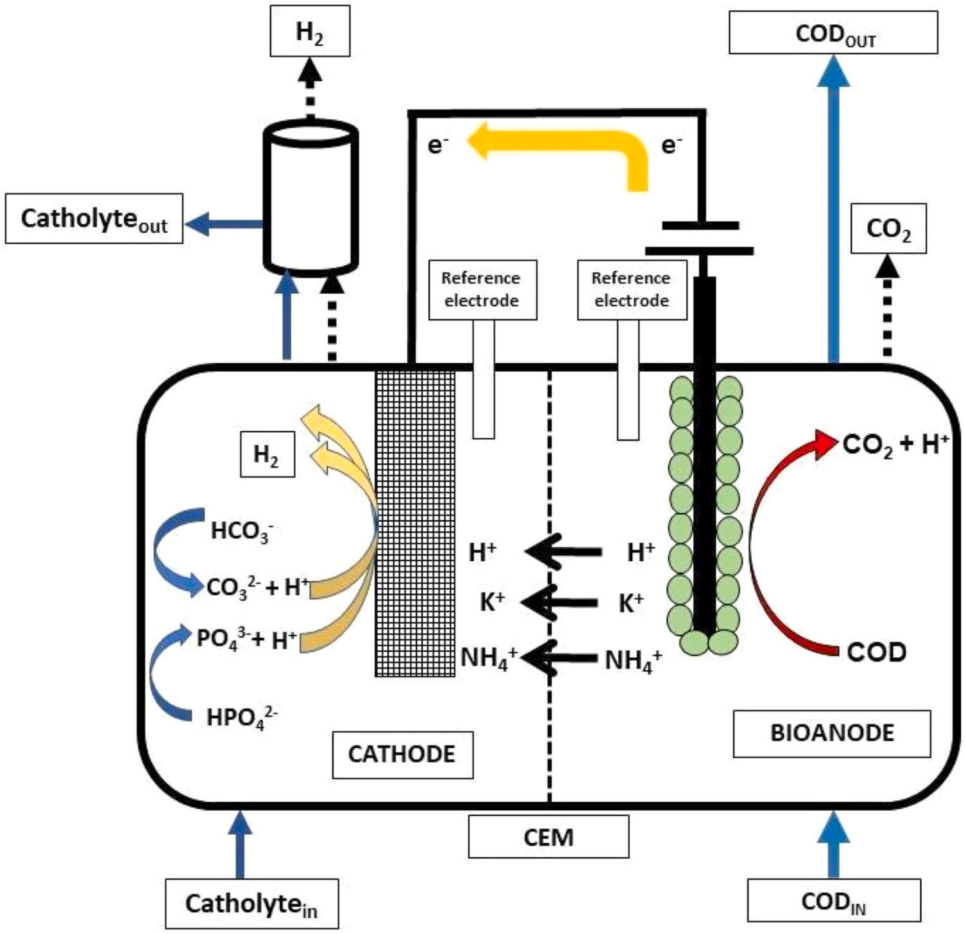

Fig. 1. Schematic representation of the two-chamber Microbial Electrolysis Cell.

together between two Plexiglas plates (Fig. 1). A Nafion® 117 cation exchange membrane (CEM) was placed between the frames. Prior to being used, the CEM was treated by boiling successively in H_2O_2 (3%, v/v), distilled water, 0.5 M H_2SO_4, and finally in distilled water again, for 2 h each. The total empty volume of each frame (i.e., of the anodic and cathodic compartments) was 0.86 L. The anodic compartment was filled with graphite granules with a diameter between 2 and 6 mm (El Carb 100, Graphite Sales, Inc, USA), while the cathodic compartment was filled with inert polyethylene support material, in order to sustain the membrane and preventing its collapse. Prior to using, the graphite granules were submerged for 24 h in 37% HCl and then for 24 h in a NaOH (1 M) solution. The washing process was repeated three times and then the granules were washed with distilled water and dried at 100 °C. The purpose of this treatment was to remove metals and eliminate any potential organic residues from the graphite material [27] Graphite granules and a graphite rod current collector (5 mm diameter, Sigma–Aldrich, Italy) were used as electrodic material in the anodic compartment while a perforated stainless-steel plate with a surface of 176.46 cm^2 was adopted as cathodic electrode material. The electrical connection between the plate and the potentiostat was guaranteed by TiO_2 wires. An Ag/AgCl reference electrode (+0.2 V vs. standard hydrogen electrode, SHE) (Amel s.r.l., Milan, Italy) was placed in each compartment in order to measure the potential of each electrode. The reactor was operated at room temperature, which was constantly maintained at 25 °C.

The anodic chamber was operated with a continuous flow of 1.44 L/d, with a solution containing: 1.250 gCOD/L (Glucose, 0.680 g/L; Sodium Acetate, 0.211 g/L; Peptone, 0.276 g/L; Yeast Extract 0.150 g/L); NH_4Cl, 0.5 g/L; $MgCl_2{\cdot}6\ H_2O$, 0.1 g/L; K_2HPO_4, 4.0 g/L; $CaCl_2{\cdot}2\ H_2O$, 0.05 g/L; 10 mL/L of a trace metals solution [28] and 1 mL/L of vitamins solution [29]. During each experimental period, a peristaltic pump continuously recirculated the anolyte (to increase the CE and the COD abatement) while the feeding solution, stored in a tedlar bag, was delivered to the reactor with a second peristaltic pump through Tygon tubes. Then a second tedlar bag was used to collect the anodic outlet. A sampling glass chamber, equipped with sampling ports sealed with butyl rubber stoppers and aluminium crimps, was placed over the chambers to sample both the liquid and gaseous phases. The anodic potential was continuously controlled with an IVIUM-n-Stat potentiostat at + 0.2 V vs SHE through a three electrodes configuration. This anodic potential was chosen following previous studies [30] in which it was demonstrated that + 0.2 V vs SHE is the break-even point for electric current and energetic consumption (a further increase of the anodic potential does not significantly increase the electric current production, but increases the energy consumption). The cathodic chamber operated both in batch and continuous flow configuration; 5 different experimental periods were performed using 5 different catholytes as reported in Table 1.

During the continuous flow phases, the feeding and discharging line at the cathode was set up in the same way as the anodic counterpart. An additional tedlar bag was placed on the top of the glass sampling chamber in order to accurately quantify the gas production. During the cathodic batch configuration, a daily spill of the catholyte was performed in order to compensate the water electro-osmotic diffusion through the CEM membrane.

2.2. MEC start-up

The inoculum used for the anodic chamber was an activated sludge collected from a full-scale wastewater treatment plant. Before the inoculation, the sludge was washed with MM and aerated in order to remove all the residual sCOD herein contained. The solids concentration in the sludge was 4.42 gVSS/L; 300 mL (35% v/v) were inoculated inside the anodic compartment which was operated in batch mode for 72 h imposing a potential of + 0.2 V vs SHE. After this phase, the sludge was considered acclimatized, and the anode bio-colonization was initiated. Then the anode electrolyte started operating in a continuous flow mode, with the feeding solution described in paragraph 2.1.

2.3. Analytical methods

H_2, CO_2, and CH_4 concentration in the gaseous samples was determined by injecting 50 μL of the gaseous sample into a Dani Master GC (Milan, Italy) gas chromatograph equipped with a thermal conductivity detector (TCD). The outlet gaseous flow rate was measured using a Ritter® milligas counter. Chemical oxygen demand (COD) was assessed by using commercial Spectroquant kit tests (Merck Millipore) and an UV–visible spectrophotometer (Shimadzu) at a wavelength of 605 nm. Electric current intensity and charge were measured automatically by the Ivium n-Stat potentiostat software while electric potentials were measured using an Amprobe AM-520-EUR multimeter. The pH and the conductivity were determined with an SI Analytics HandyLab680. The ammonium concentration was determined spectrophotometrically (420 nm) using the Nessler method. The inorganic carbon (IC) was measured with a TOC (Total Carbon Analyzer-V CSN; Shimadzu) on filtered (Ø 0.2 μm) liquid samples.

2.4. Parameters and calculations

In order to calculate the COD removal (mg/Ld), the following equation was used in which, COD_{in} and COD_{out} (mg/L) represent the influent and effluent COD concentrations, F_{in} and F_{out} (L/d) represent the influent and the effluent flow rates, respectively. The result was normalized by the anodic chamber volume (0.86 L).

$$COD_{removal}\left(mg \Big/ L \quad d\right) = \frac{F_{in} * COD_{in} - F_{out} * COD_{out}}{V} \tag{1}$$

The coulombic efficiency was calculated as follows.

$$CE(\%) = 100 * \frac{meq_i}{meq_{COD}} \tag{2}$$

In which meq_i represent the cumulative charge that has passed in the circuit and meq_{COD} represent the theoretical cumulative charge which could have been generated by the oxidation of the removed COD.

The hydrogen production rate (rH_2) was calculated as follows.

$$r_{H_2}\left(\frac{eq}{d}\right) = \frac{d\left(meq_{H_2}\right)}{d(d)} \tag{3}$$

In which $meqH_2$ are cumulative equivalents of H_2 produced, $mmolH_2$ represents cumulative moles of H_2 produced, $meq_{H_2} = 2mmol_{H_2}$ and d are the days passed during the experimental period.

The cathodic capture efficiency (CCE) was calculated as the ratio

Table 1
Catholytes composition and operation mode during the experimental periods.

	A	B	C	D	E
Operation mode	Batch	Batch	Continuous	Continuous	Batch
Catholyte	Low concentration Mineral medium (HPO_4^{2-} 23 mM) pH 7	High Concentration $H_2PO_4^-/HPO_4^{2-}$ (1.14/0.046 M) pH 5.2	Low concentration $H_2PO_4^-$ (29 mM) pH 6.1 HRT 0.78 d	High Concentration HCO_3^- (74 mM) pH 9.2 HRT 0.57 d	Low concentration HCO_3^- (1 M) pH 8.0

between the cumulative H_2 produced expressed in meq and the cumulative H_2 that could have been produced with the electric current flowing in the circuit.

$$CCE(\%) = 100 * \frac{meq_{H_2}}{meq_i} \tag{4}$$

The energetic consumptions for each process were evaluated as follows.

$$EC_{H_2}(\frac{Wh}{Ndm^3_{H_2}}) = \frac{24|\Delta V|i}{r_{H_2}24.4} \tag{5}$$

In which 24 are the hours in a day (h/d), ΔV (V) and i (A) represent the average potential difference and the average electric current registered during the experimental period, respectively. r_{H_2} represents the hydrogen production rate expressed in mol/d and 24.4 are the liters (L/mol) occupied by a mole of gas at a temperature of 25 °C.

To estimate the energetic consumption for hydrogen production considering the energy spared (1.2 kWh/kgCOD [31]) for the COD removal, taking into account that this system carries out two processes with only one energetic consumption, Eq. (5) was changed as follows.

$$EC_{COD}(\frac{Wh}{dm^3_{H_2}}) = EC_{H_2} - 1.2\eta_{COD} \tag{6}$$

In which η_{COD} represents the amount of COD removed per mole of hydrogen produced.

The overall energy efficiency was calculated as follows.

$$\eta E = \frac{|\Delta G^0_{H_2}| r_{H_2}}{3.6 * \Delta V * i * 24} \tag{7}$$

In which $\Delta G^0_{H_2}$ is the Gibbs free energy for the combustion of hydrogen (kJ/mol), r_{H_2} represents the hydrogen production rate expressed in mol/d, 3.6 is the conversion factor of kJ in Wh, 24 are the hours in a day, ΔV (V) and i (A) represent the average potential difference and the average electric current registered during the experimental period, respectively. But $\frac{r_{H_2}}{24i}$ can be rewritten as

$$\frac{r_{H_2}}{24i}(\frac{mol}{Ah}) = \frac{r_{eqH_2}}{2i24} = \frac{i_{H_2}86400}{2Fi24} \tag{8}$$

In which the hydrogen production rate is expressed as an electric current: 2 is the conversion factor of eq/mol_{H_2}, 86,400 are the seconds in a day and F is Faraday's constant (96,485 C/eq). But

$$\frac{i_{H_2}}{i} = CCE_{H_2} \tag{9}$$

Therefore, the equation number 7 can be rewritten as follows

$$\eta E = \frac{|\Delta G_{H_2}| CCE}{2|\Delta V| F} \tag{10}$$

In which $\Delta G^0_{H_2}$ is the Gibbs free energy for the combustion of hydrogen (kJ/mol), CCE_{H_2} represents the cathodic capture efficiency, 2 are the mole of electrons necessary to produce a mole of hydrogen (eq/mol_{H_2}), ΔV ($V = \frac{J}{C}$) and F is Faraday's constant (96,485 C/eq).

The following equation was used to calculate the potential loss **∑ η (V)** which represent the sum of the overpotentials.

$$\sum \eta = \Delta V_{(\exp)} - \Delta V_{(meas)} \tag{11}$$

ΔV_{exp} is the difference of potential measured between the cathode and the anode during the experiment and ΔV_{meas} represent the calculated potential difference according to the Eq. (12).

$$\Delta V_{(meas)} = E_{cath(meas)} - E_{an(meas)} \tag{12}$$

In which $E_{cath(meas)}$ and $E_{an(meas)}$ are the measured potential vs the reference electrode placed in the respective chamber. The following equation was used to calculate the cathodic potential loss ∑ η_{cat} (V) which represent the sum of the cathodic overpotential.

$$\sum \eta_{cat} = E^{meas}_{cath} - E^{th}_{cath} \tag{13}$$

In which E^{meas}_{cath} is the measured value during the experimental period whereas E^{th}_{cath} represent the theoretic value calculated with the Nernst Eq. (14).

$$E_{cath} = E^0 - \frac{RT}{2F}\ln\frac{pH_2}{[H^+]^2} \tag{14}$$

In which E° for H^+/H_2 is equal to 0 V, F is Faraday's constant (96,485 C/mol_e-), R is the universal gas constant (8.314 J/molK) and T is the temperature expressed in Kelvin. The pH_2 used is $10^{-3.1}$ atm which corresponds to 8 mM which is the maximum solubility of hydrogen in water with atmospheric pressure and normal temperature (25 °C). The same statement can be made for the anodic reaction and the anodic overpotential.

$$\eta_{an} = E_{an(meas)} - E_{an(eq)} \tag{15}$$

In case of a three electrodes configuration and a potentiostatic condition in which the anode is the working electrode, the system is working with controlled anodic overpotentials (η_{an}). Theoretically the anodic potential is calculable with Eq. (16).

$$E_{anCOD\ \ (eq)} = E^0 + \frac{RT}{8F}\ln\ln\ \ \frac{[HCO_3^-]^2 * [H^+]^9}{[CH_3COO^-]} \tag{16}$$

In which E° for HCO_3^-/CH_3COO^- is equal to + 0.187 V vs SHE, F is the Faraday's constant (96,485 C/mol_e-), R is the universal gas constant (8.314 J/molK) and T is the temperature expressed in K.

The potential losses linked to the pH gradient and to the electrolyte resistance were calculated as reported in [32].

$$\eta_{pH} = \frac{RT}{F}\ln(10^{(pH_{cathode} - pH_{anode})}) \tag{17}$$

In which, as in the Eq. (14), F is the Faraday's constant (96,485 C/mol_e-), R is the universal gas constant (8.314 J/molK) and T is the temperature expressed in Kelvin.

$$\eta_{ionic} = I_{ions}\left(\frac{1}{2}R_{anode} + \frac{1}{2}R_{cathode}\right) = I_{ions}(\frac{d_{an}}{2A\sigma_{an}} + \frac{d_{cat}}{2A\sigma_{cat}}) \tag{18}$$

I_{ions} represent the amount of charges migrated through the membrane (the value is the same of the registered electric current $\frac{C}{s}$ = A), R is the resistance of the liquid phase which can be calculated knowing the distance "d" of the electrode from the membrane (cm), the membrane's area "A" (cm^2) and the conductivity ($\frac{S}{cm}$) of the liquid phase.

5. Nitrogen mass balance

The daily nitrogen removal (ΔN; mg/d) has been evaluated by the following equation.

$$\Delta N = F_{in} * N\ \ _{in} - F_{out} * N\ \ _{out} \tag{19}$$

In which F_{in} and F_{out} (L/d) are the influent and effluent liquid flow rates, respectively. Moreover, N_{in} and N_{out} (mg/L) represent the ammonium nitrogen concentration inside the inlet and outlet of the anodic chamber. Since the nitrogen was in the form of ammonium, it could migrate through the CEM, and it was detected inside the cathodic chamber where it was recovered inside the daily spill. A small portion of ammonium is used by microorganisms for growth, it was taken into consideration for the mass balance equation according to the generic biomass composition ($C_5H_7O_2N$).

$$F_{in} * N_{in} = F_{cat} * N_{cat} + F_{out} * (N_{out} + VSS_{out}\ \ _{anode} * 0.12\frac{g_N}{g_{VSS}}) \tag{20}$$

In which F_{in} and F_{out} (L/d) are the influent and effluent liquid flow rates, respectively. Moreover, N_{in} and N_{out} (mg/L) represent the

nitrogen concentration inside the inlet and outlet of the anodic chamber. N_{cat} represent the nitrogen concentration (mg/L) inside the cathodic chamber and F_{cat} is the daily spill (L/d) from the cathodic chamber or, in case of the continuous flow configuration, the cathodic outlet flow rate; VSS_{out} is the measured concentration (mg/L) of the volatile suspended solid ($C_5H_7O_2N$) inside the anodic effluent, 0.12 is the conversion factor used for determining the ammonium nitrogen used for the biomass growth (mgN/mgVSS). Moreover, the nitrogen contribution to the total charge transport inside the MEC has been calculated by using the following equation:

$$i_N = \frac{\left[NH_4^+\right] * F_{cat} * Z * F}{86400s} \quad (24)$$

In which F_{cat} represents the daily spill (L/d) from the cathodic chamber, $[NH_4^+]$ is the ammonium concentration (mol/L) inside the cathodic chamber. Z is the amount of charge transported by the cation, F is the Faraday's constant (96,485 C/mol_e-) and 86,400 are the second in one day.

3. Results and discussion

The MEC was operated for more than 220 days without any interruption, the anodic parameters were maintained as stable as possible in order to focus the experiment on the cathodic performance. There are no duplicates because the interest is to follow the stabilization of a cell and to evaluate its behaviour and its management over the long term. As shown in Fig. S1, the electric current produced by the electroactive biofilm is stable with some fluctuation, predictable in a long-term experimentation. On the other hand, the conditions inside the cathodic chamber changed several times, starting from the composition of the catholyte to the fluid dynamic and the pHs.

3.1. Anodic chamber performance

After the start up period, the anodic electroactive biofilm worked continuously for more than 220 days maintaining the same operating conditions (i.e., OLR of 1.6 gCOD/Ld, E_{an} controlled at + 0.2 V vs SHE). The anodic chamber has been fed continuously with a solution containing on average 939 ± 129 mgCOD/L, the effluent had an average concentration of 368 ± 93 mgCOD/L, giving an average COD abatement of 61 ± 13%. The bioanode was able to treat 1.2 ± 0.3 gCOD/Ld producing an average current of 59 ± 4 mA (which corresponded to a cathodic current density of - 0.33 ± 0.08 mA/cm^2 (Fig. S1) giving an average CE of 51 ± 3%. The anodic performance did not change significantly during the whole experimental period demonstrating that the various changes carried out in the cathodic chamber did not affect

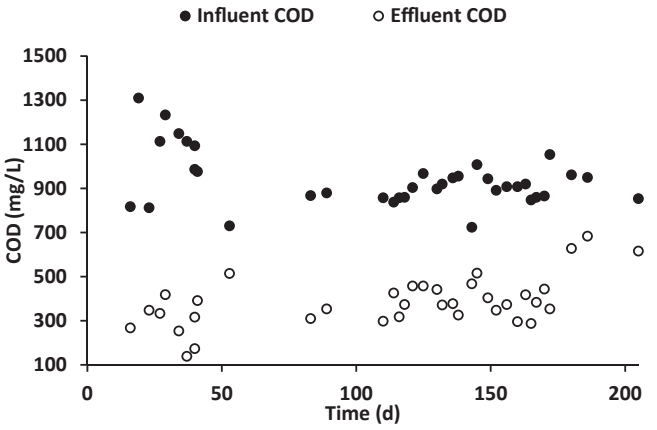

Fig. 2. Influent and effluent COD concentration measured at the inlet and outlet of the MEC anode compartment.

negatively nor positively the bioanode. The resiliency of the electroactive biofilm, shown in Fig. 2, is fundamental for processes that need to last for long periods, such as wastewater treatment.

3.2. Ammonium abatement performance

Throughout the entire experimental period, the ammonium concentration in the anodic influent and the anodic and cathodic effluents have been daily monitored. The results shown in Table 2 clearly demonstrate the capacity of the MEC to remove nitrogen from wastewaters and concentrate it in the catholyte against chemical gradient, although there are significant differences in the removal efficiency between the cathodic batch configuration (ΔN = 33 ± 1%) and the cathodic continuous flow configuration (ΔN = 59 ± 1%).

This reflects also on the amount of current counterbalanced from the ammonium's migration which was 2 ± 1 mA during the batch configuration (2.7 ± 0.1% of the total electric current) and 7 ± 2 mA using a continuous flow configuration (13 ± 3% of the total electric current). These differences in ammonium removal performance are probably since in the batch configuration the nitrogen concentration in the cathodic chamber is five times higher (442 ± 52 mgN/L) than during the continuous flow configuration (79 ± 18 mgN/L) but the spilled volume is 15 times lower than the cathodic liquid flow rate (1.050 ± 0.121 vs 0.068 ± 0.008 L/d). This gave a different chemical gradient between the two configurations, which led probably also to a retro diffusion of the ammonium cation from the cathodic to the anodic chamber. A continuous flow condition implies higher operational cost, on the contrary, a concentrated spill from the cathodic chamber gives a lower nitrogen removal from the treated synthetic wastewater.

3.3. Cathodic chamber performance: 23 mM HPO_4^{2-} buffer (pH 7) in batch configuration (A)

As first catholyte, the same mineral medium (MM) was used in the feeding solution for the bioanode. Inside the MM were present 4 g/L K_2HPO_4, which is used to maintain the pH stable around physiological values. Working with a weak buffer ($[HPO_4^{2-}]$ = 23 mM) in a configuration such as this inevitably leads to a fast alkalinization (3 days) of the cathodic compartment due to the consumption of protons for the hydrogen production that are not balanced due to migration of cations different from protons from the anodic chamber. This migration through the CEM is necessary to maintain the electroneutrality inside the chambers. The relative high concentration of cations inside the MM such as calcium (4.5 mM), magnesium (10.5 mM), potassium (46 mM), and sodium (2.5 mM) limit the migration and refuelling of protons, which have a concentration inside the anolyte between 10^{-7} and $10^{-5.5}$ mol/L. As shown in Fig. S2, a quick pH increase led to obtain a steady pH value of 13.77 ± 0.03: in accordance with Nernst's Eq. (14) this corresponds to a decrease of the equilibrium cathodic potential to – 789.6 mV, but due potential losses the real cathodic potential results higher. In fact, the

Table 2
impact of different composition and management conditions of the catholyte on the nitrogen mass balance.

Experimental period	A	B	C	D	E
N_{in} (mgN/d)	95 ± 1	99 ± 1	116 ± 1	127 ± 1	103 ± 1
N_{out} (mgN/d)	61 ± 1	36 ± 1	54 ± 1	45 ± 1	42 ± 1
N_{outVSS} (mgN/d)	13 ± 1	12 ± 2	10 ± 1	9 ± 1	20 ± 2
N_{cat} (mgN/d)	1.5 ± 0.1	26 ± 4	90 ± 1	89 ± 1	13 ± 1
Nitrogen removal (ΔN %)	35 ± 2	64 ± 1	54 ± 1	65 ± 1	59 ± 1
i_N (mA)	0.12 ± 0.01	2.1 ± 0.3	7.2 ± 0.1	7.1 ± 0.1	1.0 ± 0.1
I_N/i_{TOT} (%)	0.17 ± 0.01	3.6 ± 0.5	12.8 ± 0.1	12.2 ± 0.1	1.8 ± 0.1

average measured cathodic potential was − 1.1 ± 2 V (vs SHE). In this condition the obtained r_{H_2} was 37 ± 4 meq/d (0.21 ± 0.02 meq /cm^{2}d) corresponding to a CCE of 67 ± 5%. The relatively low CCE was probably influenced by the high pH generated by the pH split phenomenon therefore a different catholyte with a higher buffer concentration was introduced as catholyte.

3.4. Cathodic chamber performance: phosphate buffer in batch configuration $H_2PO_4^-/HPO_4^{2-}$ buffer solution (1.140 M: 0.046 M; initial pH 5.2) (B)

To avoid such a rapid alkalinization such as in the previous case (A; HPO_4^{2-} 23 mM), a concentrated buffer solution was used as catholyte ([HPO_4^{2-}] = 46 mM and [$H_2PO_4^-$] = 1.140 M). The initial concentrations were calculated considering an average electric current of 59 ± 4 mA (53 meq are daily reducing the same amount of H^+), which means that 1.1 moles of $H_2PO_4^-$ are necessary in 1 L of catholyte, in order to last at least 21 days. The initial pH of the catholyte solution resulted 5.21, after 19 days of operation the catholyte pH reached the value of 13, indicating the complete consumption of the solution buffer capacity. Therefore, the catholyte was removed and substituted by fresh catholyte solution; as reported in Fig. S3, which shows the catholyte pH time course, a reproducible result was obtained (between day 100 and 118) in terms of buffer capacity consumption. Even though the pH increase, during the two batch periods, the average hydrogen production rate r_{H_2} resulted of 44 ± 2 meq/d which corresponded to a specific production rate, i.e., the production rate referred to the cathodic electrode surface of 0.25 ± 0.01 meq/cm^{2}d. Moreover, considering the average current flowing in the circuit, a cathode capture efficiency (CCE) of 86 ± 3% was obtained, a higher value with respect to the previous condition with the mineral medium catholyte. This effect is probably due to the catalytic effect of $H_2PO_4^-/HPO_4^{2-}$ buffers described in literature [26]. This effect was visible only in this condition and not in condition (A) because the concentration was two orders of magnitude higher (1.140 M $H_2PO_4^-$ and 0.023 M HPO_4^{2-}, respectively). The cathodic potential decreased along with the increase of the pH value, as predicted by the Nernst's Eq. (14), reaching a ΔV of – 2.79 V (starting from −1.23 V). Which means that even if (as expected) the H_2 production did not change, the energetic cost of the process increased by the 228 ± 21% during this experimental period.

3.5. Cathodic chamber performance: 0.029 M $H_2PO_4^-$ pH 6.1 solution in continuous flow configuration (C)

During the third operational period, a continuous flow configuration was adopted in the cathodic chamber by feeding a 29 mM $H_2PO_4^-$ buffer solutiouren at a flow rate of 1.05 L/d to achieve a stable pH value of around 7.72 ± 0.48. Those parameters (initial concentration and flow rate) were set after titration of the buffer solution (equivalence point reached after adding 1.2 eq/L), taking into account a stable electric current of 59 ± 4 mA that generated constantly alkalinity inside the cathodic chamber. Indeed, considering the complete charge transfer through the CEM membrane by other cations different from protons, an electric current of 59 ± 4 mA theoretically generates a maximum of 53 ± 3 millimoles of alkalinity per day. Stable pH and cathodic potential were obtained therefore, as reported in Fig. S4, it has been proven that it is possible to stop the increase of the cathodic pH by working in a continuous flow condition. As a result of this new configuration, the cathodic potential was stable at around - 0.91 ± 0.09 V vs SHE, while the average r_{H_2} was of 17 ± 3 meq/d or 0.10 ± 0.02 meq/cm^{2}d considering the cathodic electrodic surface, moreover the average CCE resulted 54 ± 6%. The obtained stable pH around 7.3 ± 0.2 allowed the proliferation of hydrogenophilic microorganisms like methanogens (r_{CH_4} = 1.4 meq/d), this led to a consumption of the produced hydrogen. To prevent contamination and above all, to guarantee maximum production of hydrogen without impurities, sterile conditions should have been guaranteed, but this would mean higher operational costs. So, a different buffer solution, or a different pH is needed in order to preserve the hydrogen produced by the system.

3.6. Cathodic chamber performance: 0.074 M HCO_3^- pH 9.2 solution in continuous flow configuration (D)

Since phosphate is a non-renewable and expensive chemical, a more sustainable weak acid able to catalyse hydrogen production at the cathodic side of a MEC is represented by bicarbonate [23,26] even if it could represent a carbon source for autotrophic microorganisms. A catholyte, consisting of a buffer solution containing HCO_3^-, has a higher pH (> 9), which will inhibit most hydrogenophilic microbial metabolism. The catholyte solution consisting of HCO_3^- 74 mM was continuously fed with a flow rate of 1.47 L/d. Also in this case, the parameters (flow rate, HCO_3^- concentration and pH) were calculated knowing the amount of alkalinity generated inside the cathodic chamber (53 meq/d). As shown in Fig. S5 the cathodic pH and potential remained stable throughout the whole duration (40 days) of the experiment around 9.8 ± 0.2 and − 0.91 ± 0.09 V vs SHE, respectively. A constant pH leads to a constant cathodic potential which means a constant energetic consumption, moreover, due the catalytic effect of bicarbonate (which is predominant around pH values of 8) is important to have a pH as near as possible to 8. In this period the r_{H_2} resulted on average 33 ± 2 meq/d (0.19 ± 0.01 meq/cm^{2}d) while the CCE = 65 ± 3%. The high pH and the low HRT did not permit any contamination by methanogenic microorganisms; therefore, the hydrogen production rate resulted significantly higher than the one registered during the previous experimental period (i.e., buffer solution of $H_2PO_4^-$ fed continuously; 17 ± 3 meq/d). Interestingly, the cathodic potential was similar to the one obtained previously, even if the pH was higher (7.3 ± 0.2 vs 9.8 ± 0.2), which resulted in line with the reported catalytic effect of bicarbonate in the literature [23]. Fig. 3 shows the variations of the cathodic potential during the 5 operating periods. It's clear to see that a lower concentration of proton donors decreases the cathodic potential. Moreover, at the same pH values, the catalytic effect is more prominent with the bicarbonate solution because, for an identical production of hydrogen, the cathodic potential is systematically less negative in the presence of a bicarbonate solution than with a phosphate solution. This could be explained by the lower K_a value of the monohydrogen phosphate deprotonation (K_{a3}:4,5 ×10^{-13} vs K_{a2}: 5,60 ×10^{-11}) with respect to the

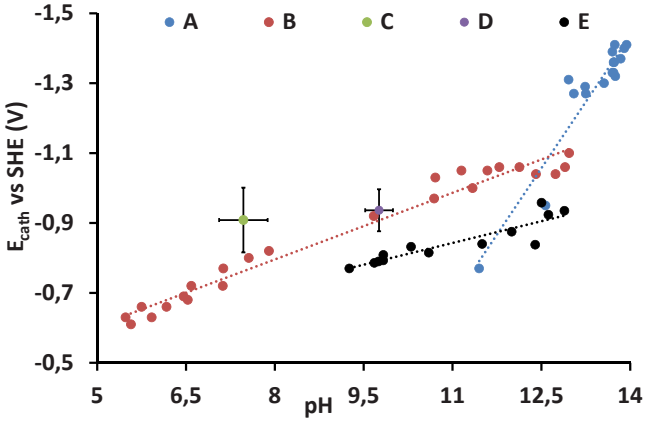

Fig. 3. Cathodic potential and pH measured during the 5 experimental periods (with an average electric current of 59 ± 4 mA). A, low concentration HPO_4^{2-} buffer in batch configuration; B, high concentration $H_2PO_4^-$ buffer in batch configuration; C, low concentration $H_2PO_4^-$ buffer in continuous flow configuration; D, low concentration HCO_3^- buffer in continuous flow configuration; E, high concentration HCO_3^- buffer in batch configuration.

K_a value of bicarbonate deprotonation.

$$H^+ + HPO_4^{2-} + e^- \rightarrow H_2 + PO_4^{3-}$$

$$H^+ + HCO_3^- + e^- \rightarrow H_2 + CO_3^{2-}$$

3.7. Cathodic chamber performance: high concentration HCO_3^- buffer in batch configuration (E)

In order to compare the results obtained with the $H_2PO_4^-$ buffer in batch configuration and to confirm the catalytic effect of bicarbonate in the electrochemical production of hydrogen; as reported in [23], the same 1 M HCO_3^- buffer solution (pH 8) was introduced in the cathodic chamber in a batch configuration. As reported in Fig. S6, cathodic pH and potential increased over time due to the usual alkalinisation of the catholyte. In this configuration the average r_{H_2} was of 39 ± 1 meq/d (0.220 ± 0.006 meq/cm^{2}d) while the CCE was 79 ± 1%, this performance is better than the one obtained with a continuous flow configuration, probably due to a loss of solubilized hydrogen inside the outlet and some leakages of the flow line. Interestingly, even if the pH raised from a value of 8.7 to 13.1, the cathodic potential decreased only from -0.77 V vs SHE to – 0.96 V vs SHE (giving an increase of 19.6% of the cell voltage which translates into the same level of increase of the cost price); those values are lower than the one predictable with the Nernst's Eq. (14). Fig. 4 shows how the cathodic potential changed while the pH was changing during the two batch conditions (B, concentrated $H_2PO_4^-$ solution in batch configuration; E, concentrated HCO_3^- solution in batch configuration), indicating that the measured cathodic potentials are significantly different than the ones predictable with the Nernst's equation. The slopes are comparable but the difference between the three functions can be attributed to the overpotentials of the semi reactions.

3.8. Characterization of the MEC's potential loss

During the whole experimental period both the anode and the cathode potentials were monitored and measured to obtain a more complete picture of the MEC energetic performance. It is important to consider that the feeding solution used as anolyte had a composition and a pH that did not change significantly. The influent and effluent anolyte pH decreased on average from 6.8 ± 0.1 to 6.1 ± 0.2, indicating a partial acidification due to the generation (i.e. COD oxidation) and accumulation of protons. The feeding solution supply, the anodic conditions in terms of fixed potential and finally anodic current performance were unaltered during each experimental period. For this reason, also the conductivity of the anolyte did not change significantly being on

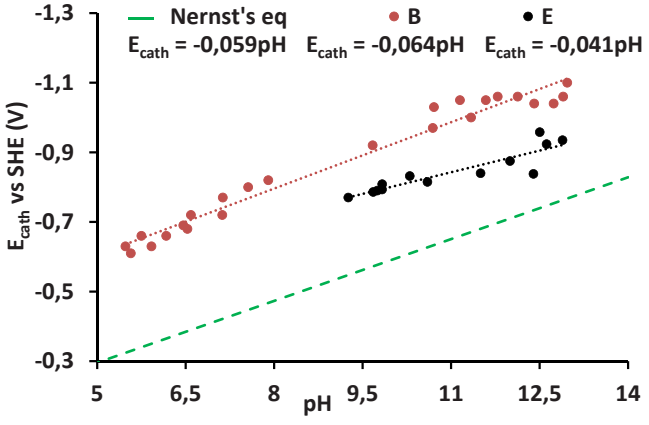

Fig. 4. Cathodic potential and pH registered during the 2 experimental periods in batch configuration. B, high concentration $H_2PO_4^-$ buffer; E, high concentration HCO_3^- buffer.

average 4.0 ± 0.5 mS/cm. The anodic potential was controlled by a potentiostat with a three-electrode configuration at + 0.2 V vs SHE, therefore, only the cathodic potential, which represented the counter electrode of the cell, was able to change significantly as a function of the operating conditions. Moreover, the cathodic overpotential was calculated following Eqs. (14) and (15). Since the $[H_2]$ was considered stable at 0.8 mM, the theoretic cathodic potential changed along with the pH (from E_{cath} = – 0.46 ± 0.04 V vs SHE for pH 9.3 ± 0.4 during B period to E_{cath} = – 0.70 ± 0.06 V vs SHE with pH 13.4 ± 0.6 during A period). The cathodic potential loss (or overpotential), reported in Fig. S7, variated from 0.2 ± 0.1 V to 0.5 ± 0.1 V demonstrating that with a medium size stainless steel electrode (176 cm^2) inside a 0.86 L chamber the overpotential is around 33 – 55% of the measured cathodic potential. Stainless steel is considered a good material for electrochemical hydrogen production, but there are many more expensive catalysts (made with Pt or Pt/C, Pd, MoS_2) capable of producing H_2 with lower overpotentials [33]. Every cathode batch operation mode allowed for cation concentration inside the cathodic chamber; this led to a high conductivity of the catholyte and therefore a low resistance inside the cathodic chamber which can improve its efficiency and performance. There are several strategies that can be employed to reduce the internal resistance of a MEC, like geometry improvement: higher surface area to volume ratio, which allows for better distribution of current and more efficient electron transfer or increasing the number and size of electrodes can also help in reducing internal resistance by providing more pathways for electron flow. A second strategy could be represented by reducing the distance between electrodes and increasing conductivity in the electrolytes. A shorter distance between the electrodes reduces the path length for electron transfer, thereby decreasing the resistance encountered by the electrons and, higher conductivity facilitates faster ion movement and better electron transfer between the electrodes, resulting in reduced internal resistance. For those reasons, the calculations gave lower ionic losses during the three batch periods (A, B and E) than the one calculated for the periods C and D (characterized by a continuous flow condition for the catholyte) during which the catholyte's conductivity was on average only 8.5 ± 0.7 mS/cm. The ionic losses were calculated following the Eq. 17 reported in [32], and resulted in 0.12 ± 0.01, 0.12 ± 0.01 and 0.11 ± 0.01 V for the A, B and E periods, respectively. On the other hand, the batch conditions led to very alkaline cathodic pHs and subsequently to a relative high pH split between anolyte and catholyte (6.1 ± 0.2 vs 13.2 ± 0.5, respectively). A stable and not highly alkaline pH obtained with the continuous flow configuration allowed to lower pH gradient loss (Fig. S8). Interestingly, cathodic batch operation mode resulted in higher pH gradient losses but lower ionic losses, while on the contrary, the cathodic continuous flow operation mode allowed to decrease pH gradient losses while increasing voltage losses caused by ionic losses (i.e. a lower conductivity of the catholyte). In fact, working with concentrated buffer solution in batch conditions leads to a constant high conductivity, lowering the potential losses. Thereby, no significant difference was calculated between pH gradient and ionic losses of the B, C, D and E periods and their sum resulted always around 0.32 ± 0.02 and 0.40 ± 0.02 V. On the other hand, Table 3 shows there is no significant difference of the cell overpotential between the batch or continuous flow configuration while using $H_2PO_4^-$ buffer solution as catholyte (periods B and C had 0.9 ± 0.1 V cell overpotential). A different result was obtained by changing configuration while using HCO_3^- buffer solutions; the cell overpotential dropped from 1.1 ± 0.1 to 0.6 ± 0.1 V. Those results were not explained by pH gradient and ionic losses calculations but could be explained by the catalytic effect of concentrated HCO_3^- reported in [23]. This explains also the low cathodic potential loss during the last (E) period, which was on average 0.2 ± 0.1 V. Those promising results obtained during the last experimental period (lowest ΔV, cathodic potential loss and cell overpotential) demonstrate that even if the B period produced more hydrogen, the E period was able to produce hydrogen with a lower

Table 3
Potential loss of the system during each experimental period.

Experimental period	A	B	C	D	E
i (mA)	70 ± 1	57 ± 2	56 ± 3	61 ± 1	68 ± 4
ΔV (V)	- 2.0 ± 0.2	- 2.0 ± 0.1	- 2.1 ± 0.2	- 2.3 ± 0.1	- 1.7 ± 0.1
E_{cath} (V vs SHE)	- 1.1 ± 0.1	- 0.9 ± 0.1	- 1.0 ± 0.1	- 1.0 ± 0.1	- 0.9 ± 0.1
η_{cath} (V)	0.3 ± 0.1	0.4 ± 0.1	0.5 ± 0.1	0.5 ± 0.1	0.3 ± 0.1
η_{pH} (V)	0.4 ± 0.1	0.2 ± 0.1	0.2 ± 0.1	0.2 ± 0.1	0.3 ± 0.1
η_{ionic} (V)	0.1 ± 0.1	0.1 ± 0.1	0.2 ± 0.1	0.2 ± 0.1	0.1 ± 0.1
∑ η (V)	0.7 ± 0.1	0.9 ± 0.1	0.9 ± 0.2	1.1 ± 0.1	0.6 ± 0.1

energetic loss. Fig. 5 shows how the cell overpotentials are distributed and, interestingly, the E period is the one with the lowest cell overpotential even if the pH and the ionic overpotentials are comparable to the ones measured and calculated during the other periods. The "unknown" over potential (in which are considered the membrane resistance Nafion 117 0.16 Ω*cm [34] and the activation losses/electrons transfer resistance) can be significantly lower giving a lower cell overpotential and therefore a lower energetic consumption. Ohmic losses and activation losses are directly related to the type of used materials, operating temperature and contact area [35]. Increasing the temperature will inevitably increase the operational costs.

Using different geometries (i.e., tubular) or different materials with better performances and higher contact area than graphite granules could represent a solution, but the investment cost will inevitably rise. The graphite granules were used as electrodic material for their compatibility with biofilms formation, as well as for their relatively good electrochemical properties such as conductivity and low degradability at the used potentials and, more importantly, for their low cost. Moreover, it was demonstrated that an anode placed in between a two-side cathode reduces the overpotentials of an electrochemical system by lowering the average distance between an anodic side and one cathode; in this case a single cathodic chamber was used which probably has increased the cell overpotential. Is important to remember that one of the biggest problems of MECs is the low conductivity (thus high resistance) of the real wastewaters.

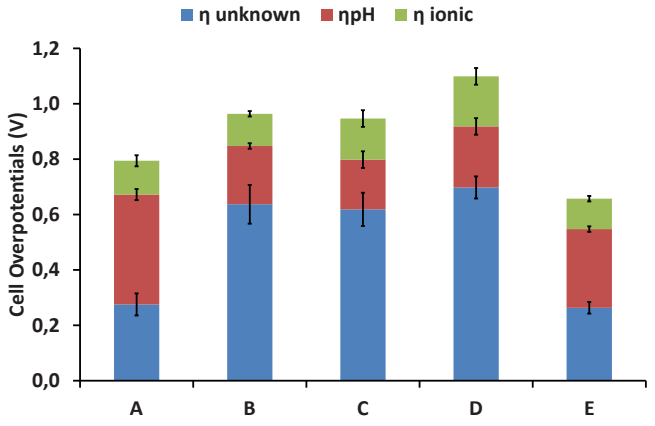

Fig. 5. Cell overpotentials calculated for the 5 experimental periods. A, low concentration HPO_4^{2-} buffer in batch configuration; B, high concentration $H_2PO_4^-$ buffer in batch configuration; C, low concentration $H_2PO_4^-$ buffer in continuous flow configuration; D, low concentration HCO_3^- buffer in continuous flow configuration; E, high concentration HCO_3^- buffer in batch configuration.

3.9. Energetic performance

The energetic performances have been constantly monitored throughout the various reactor configurations; the main parameters are shown in the Table 4. Peak ηE was achieved with configuration B, thanks to a high CCE (86 ± 3%) probably due to the catalytic effect of concentrated $H_2PO_4^-$, this confirms the logical necessity of producing hydrogen with the best cathodic efficiency. Stainless steel is a good material to perform this electrochemical reaction, the high conductivity and the presence of a proton donor enhance this performance.

Each experimental period had a good energetic efficiency (up to 68 ± 5%), which means that in the worst scenario (i.e., configuration C with buffer solution containing $H_2PO_4^-/HPO_4^{2-}$ with a continuous flow configuration), this MEC abated COD recovering in form of hydrogen the 40 ± 4% of the energy spent to supply the process. These promising results could lead to a more sustainable wastewater treatment process, which nowadays does not recover the energy of their COD content. The best EC and, logically having the same anodic performance, the best EC_{COD} performance were instead obtained with configuration E (i.e., buffer solution containing 1 M of bicarbonate in batch configuration; also, configuration B was very good i.e., batch configuration using a buffer solution of $H_2PO_4^-/HPO_4^{2-}$) thanks to a low ΔV and a high r_{H_2}. This confirms the importance of a system with low potential loss, high cathodic potential, and high conversion of electricity in hydrogen (high CCE). The bicarbonate buffer solution permitted to obtain all those three parameters, confirming what was reported in[23]. There is a thermodynamic limit for hydrogen production under which it is not possible to produce it, therefore, to further reduce the energetic consumption it is mandatory to couple this process with a renewable energy production. All EC_{COD} values, which take into account the energy that a wastewater treatment plant would spend to remove the COD abated by the MEC, except configuration C and D, are lower than the energy consumption of benchmark value for industrial alkaline electrolysers (4.5 kWh/Nm^3H_2), meaning that a MEC could lower current energy consumption for H_2 production by combining it with COD abatement. Moreover, it was demonstrated that the MEC did work efficiently for more than 220 days proving once more its durability. This promising result should be transferred in a pilot scale reactor and, if confirmed, could lead to an eco-friendly low-cost production of hydrogen.

3.10. Comparison of the study performances with literature studies

Table 5 presents the results published in the literature regarding hydrogen production through MEC. This is done to compare them with the results of periods B and E in the current study. Despite differences in the configuration of the MEC cathodic chamber, the results show comparable outcomes in terms of COD removal efficiency and anodic and cathodic coulombic efficiency.

Table 4
Energy efficiency **(ηE)**, Energy Consumption **(EC)**, Energy Consumption considering COD abatement **(EC_{COD})** in the different configurations: A, low concentration HPO_4^{2-} buffer in batch configuration; B, high concentration $H_2PO_4^-$ buffer in batch configuration; C, low concentration $H_2PO_4^-$ buffer in continuous flow configuration; D, low concentration HCO_3^- buffer in continuous flow configuration; E, high concentration HCO_3^- buffer in batch configuration.

Parameters	Configuration				
	A	B	C	D	E
ΔV (V)	- 2.0 ± 0.2	- 2.0 ± 0.1	- 2.1 ± 0.2	- 2.3 ± 0.1	- 1.7 ± 0.1
CCE (%)	67 ± 5	86 ± 3	37 ± 5	60 ± 3	79 ± 6
ηE (%)	48 ± 5	68 ± 5	40 ± 4	48 ± 2	55 ± 8
EC (kWh/Nm^3H_2)	6.70 ± 0.12	5.22 ± 0.09	12.79 ± 0.32	8.29 ± 0.22	4.46 ± 0.18
EC_{COD} (kWh/kgCOD)	4.39 ± 0.12	3.17 ± 0.08	8.14 ± 0.18	5.60 ± 0.19	1.77 ± 0.07

Table 5
MECs performance in literature for H_2 Production.

REF.	CURRENT DENSITY	COD Removal (%)	CE (%)	CATHODIC CONFIGURATION.	H_2 Production rate	CCE (%)	ηE (%)
c.s.*	59 ± 5 A/m^3	61 ± 13	51 ± 3	Abiotic (operating period E)	0.56 m^3/m^{3}d	79 ± 1	55 ± 8
c.s.*	59 ± 5 A/m^3	61 ± 13	51 ± 3	Abiotic (operating period B)	0.62 m^3/m^{3}d	86 ± 3	68 ± 5
[36]	163 A/m^3	88 ± 3	47.2	Abiotic	1.04 m^3/m^{3}d	57 ± 5	89
[37]	312 ± 9 A/m^3	94 ± 2	75 ± 4	Biotic – Single Chamber	4.18 ± 1 m^3/m^{3}d	89 ± 4	94.1 ± 3.3
[38]	26 ± 2 A/m^3	50	62 ± 6	Abiotic	0.24 ± 0.01 m^3/m^{3}d	84 ± 4	-
[39]	10 ± 1 A/m^3	-	89 ± 6	Abiotic	0.42 ± 0.04 m^3/m^{3}d	79 ± 2	77 ± 2
[40]	75 A/m^3	-	87 ± 10.2	Abiotic	0.22 ± 0.02 m^3/m^{3}d	39 ± 3	40 ± 4

* current study

Regarding COD removal, the compared studies were almost in line with the average performance of the bioanode described in the present study. However, significant differences have been highlighted in the compared studies, indeed, study [37] achieved a value of 94% ± 2%, while [38] reported a considerably lower value of 50%. The notable difference can primarily be attributed to the use of a pure culture of Geobacter sulfurreducens as an inoculum in [37]. This microorganism is well-known for its electroactive properties and can produce high power densities at moderate temperatures. In contrast, the authors of [38] used a mixed microbial culture from the sugar industry wastewater, which seemed to affect the reactor's performance. Three studies [36,37] achieved better performances in terms of volumetric current density compared to the average value of 59 A/m^3 obtained during operating periods B and E. In these studies, current densities reached significantly higher values, corresponding to 163 and 312 A/m^3. A possible explanation for these results can be attributed to the use of catalytic materials for the hydrogen evolution reaction. For instance, in [36], a modified electrode with polyaniline (PANI)/multi-walled carbon nanotube (MWCNT) was investigated as the electrodic material, while in [37], a Ni mesh cathode was prepared to enhance the catalytic activity for hydrogen production. Furthermore, when comparing the volumetric hydrogen production rates obtained in [36] and [37], higher values of hydrogen production (1.04 and 4.18 ± 0.98 m^{3}H$_2$/m^{3}d) were achieved, compared to the values of 0.55 and 0.66 m^{3}H$_2$/m^{3}d obtained during the present study (operating periods E and B). Although the performances of operating periods B and E in this study were lower than those of [36] and [37], a comparison with other literature studies [38–40] reveals slightly higher performances in the present study. In fact, the volumetric hydrogen production of 0.55 and 0.66 m3H2/m3d is in line with the values of 0.24 m^{3}H$_2$/m^{3}d [38], 0.44 m^{3}H$_2$/m^{3}d [39], and 0.22 m^{3}H$_2$/m^{3}d [40] reported in those studies. It's worth noting that all of these studies [38–40] involved the use of different abiotic materials synthesized to stimulate the hydrogen production reaction.

4. Conclusions

The herein study confirmed the good potential of Microbial Electrolysis Cells in coupling COD oxidation at the bioanode with green hydrogen production at the cathode in a single biobased process. Indeed, the bioanode provides a stable source of electrons to the cathodic reaction without being significantly affected by catholyte composition and operation mode, i.e. the electric current produced by the electroactive biofilm through the COD oxidation was on average 59 ± 4 mA corresponding to a coulombic efficiency of 51 ± 23%. The first tested catholyte, consisting in the mineral medium of the feeding solution (operating period A) resulted in energy consumption of 6.70 ± 0.12 kWh/Nm^{3}H$_2$ probably due to its low buffer potential and pH increase which affected the cell voltage of the MEC. Being the hydrogen production reaction more favourable at potential close to 0 V vs SHE, the $H_2PO_4^-$/HPO_4^{2-} buffer solution gave better performance, giving the highest hydrogen production rate r_{H_2} of 44 ± 2 meq/d and the highest cathodic coulombic efficiency, with an average value of 86 ± 3% confirming previous results study [23]. However, using the $H_2PO_4^-$/HPO_4^{2-} buffer solution in continuous flow mode to keep the pH at a value of 7.3 ± 0.2, a contamination of methanogens lowered H_2 production rate to 17 ± 3 meq/d increasing the energy consumption of the process to 12.79 ± 0.32 kWh/Nm^{3}H$_2$. The utilization of a more sustainable HCO_3^- buffer solution under continuous flow condition allowed the H_2 production at higher pH (i.e., 9.8 ± 0.2) maintaining stable the cathodic potential at - 1.0 ± 0.1 V vs SHE, confirming the catalytic effect of bicarbonate for the hydrogen production reported in the literature [23]. The higher pH reached by the HCO_3^- catholyte (9.8 ± 0.2 vs 7.3 ± 0.2) inhibited the hydrogenophilic metabolisms giving lower hydrogen losses (r_{H_2} 17 ± 3 meq/d vs 33 ± 2 meq/d) but led to a slightly higher pH potential loss (0.22 ± 0.01 vs 0.18 ± 0.01 V). Interestingly both catholytes dosed under continuous flow configuration led in both cases to a loss of hydrogen due to its solubilization inside the cathodic outlet resulting in relatively low CCE. At last, following the promising results obtained with a HCO_3^- buffer solution, a catholyte containing 1 M HCO_3^- in batch configuration was assessed. This last catholyte permitted to obtain H_2 at a r_{H_2} of 39 ± 1 meq/d with the lowest energetic consumption (i.e., 4.46 ± 0.18 kWh/Nm^{3}H$_2$), comparable with the energetic consumption of the commercial electrolyzers (4.5 kWh/Nm^{3}H2) This interesting result was obtained probably due to the relative low cell overpotential, in fact, calculating the various contributions of the potential losses, this catholyte carried out the hydrogen production with a global overpotential ($\sum\eta$)of 0.6 ± 0.1 V (of which ηpH 0.28 ± 0.01 and ηionic 0.11 ± 0.01).

CRediT authorship contribution statement

Lorenzo Cristiani: Investigation, Writing – original draft, Writing – review & editing. **Marco Zeppilli**: Supervision, Writing – review & editing. **Damiano Feriaud**: Investigation. **Clara Marandola**: Investigation. **Marco Petrangeli Petrangeli Papini**: Supervision. **Serge Da Silva**: Supervision. **Benjamin Erable**: Supervision. **Marianna Villano**: Supervision, Writing – review & editing.

Declaration of Competing Interest

The authors declare that they have no known competing financial interests or personal relationships that could have appeared to influence the work reported in this paper.

Data availability

The data that has been used is confidential.

Acknowledgments

The authors acknowledge prof. Mauro Majone for his fruitful support in scientific discussion of the results.

Appendix A. Supporting information

Supplementary data associated with this article can be found in the

online version at doi:10.1016/j.jece.2023.111782.

References

[1] Y. Gao, X. Gao, X. Zhang, The 2 °C Global Temperature Target and the Evolution of the Long-Term Goal of Addressing Climate Change—From the United Nations Framework Convention on Climate Change to the Paris Agreement, Engineering 3 (2017) 272–278, https://doi.org/10.1016/J.ENG.2017.01.022.

[2] E.S. Heidrich, S.R. Edwards, J. Dolfing, S.E. Cotterill, T.P. Curtis, Performance of a pilot scale microbial electrolysis cell fed on domestic wastewater at ambient temperatures for a 12month period, Bioresour. Technol. 173 (2014) 87–95, https://doi.org/10.1016/j.biortech.2014.09.083.

[3] J.D. Holladay, J. Hu, D.L. King, Y. Wang, An overview of hydrogen production technologies, Catal. Today 139 (2009) 244–260, https://doi.org/10.1016/j.cattod.2008.08.039.

[4] C. Koroneos, A. Dompros, G. Roumbas, N. Moussiopoulos, Life cycle assessment of hydrogen fuel production processes, Int. J. Hydrog. Energy 29 (2004) 1443–1450, https://doi.org/10.1016/j.ijhydene.2004.01.016.

[5] J. Turner, G. Sverdrup, M.K. Mann, P.-C. Maness, B. Kroposki, M. Ghirardi, R. J. Evans, D. Blake, Renewable hydrogen production, John, Arch. Thermodyn. 32 (2007), https://doi.org/10.1002/er.1372.

[6] H. Janssen, J.C. Bringmann, B. Emonts, V. Schroeder, Safety-related studies on hydrogen production in high-pressure electrolysers, Int. J. Hydrog. Energy 29 (2004) 759–770, https://doi.org/10.1016/j.ijhydene.2003.08.014.

[7] B.E. Logan, D. Call, S. Cheng, H.V.M. Hamelers, T.H.J.A. Sleutels, A.W. Jeremiasse, R.A. Rozendal, Microbial electrolysis cells for high yield hydrogen gas production from organic matter, Environ. Sci. Technol. 42 (2008) 8630–8640, https://doi.org/10.1021/es801553z.

[8] H. Liu, S. Grot, B.E. Logan, Electrochemically assisted microbial production of hydrogen from acetate, Environ. Sci. Technol. 39 (2005) 4317–4320, https://doi.org/10.1021/es050244p.

[9] R.A. Rozendal, H.V.M. Hamelers, G.J.W. Euverink, S.J. Metz, C.J.N. Buisman, Principle and perspectives of hydrogen production through biocatalyzed electrolysis, Int. J. Hydrog. Energy 31 (2006) 1632–1640, https://doi.org/10.1016/j.ijhydene.2005.12.006.

[10] P. Chong, B. Erable, A. Bergel, Microbial anodes: What actually occurs inside pores? Int. J. Hydrog. Energy 44 (2019) 4484–4495, https://doi.org/10.1016/j.ijhydene.2018.09.075.

[11] L. Cristiani, J. Ferretti, M. Majone, M. Villano, M. Zeppilli, Autotrophic Acetate Production under Hydrogenophilic and Bioelectrochemical Conditions with a Thermally Treated Mixed Culture, Membr. (Basel) 12 (2022), https://doi.org/10.3390/membranes12020126.

[12] Charles Rino, The Theory of Scintillation with Applications in Remote Sensing, Wiley-IEEE Press, 2011. https://www.wiley.com/en-sg/The+Theory+of+Scintillation+with+Applications+in+Remote+Sensing-p-9780470644775.

[13] A. Kadier, Y. Simayi, M.S. Kalil, P. Abdeshahian, A.A. Hamid, A review of the substrates used in microbial electrolysis cells (MECs) for producing sustainable and clean hydrogen gas, Renew. Energy 71 (2014) 466–472, https://doi.org/10.1016/j.renene.2014.05.052.

[14] P. Pandey, V.N. Shinde, R.L. Deopurkar, S.P. Kale, S.A. Patil, D. Pant, Recent advances in the use of different substrates in microbial fuel cells toward wastewater treatment and simultaneous energy recovery, Appl. Energy 168 (2016) 706–723, https://doi.org/10.1016/j.apenergy.2016.01.056.

[15] D. Pant, G. Van Bogaert, L. Diels, K. Vanbroekhoven, A review of the substrates used in microbial fuel cells (MFCs) for sustainable energy production, Bioresour. Technol. 101 (2010) 1533–1543, https://doi.org/10.1016/j.biortech.2009.10.017.

[16] R. Rousseau, S.F. Ketep, L. Etcheverry, M.L. Délia, A. Bergel, Microbial electrolysis cell (MEC): A step ahead towards hydrogen-evolving cathode operated at high current density, Bioresour. Technol. Rep. 9 (2020) 100399, https://doi.org/10.1016/j.biteb.2020.100399.

[17] R. Rousseau, L. Etcheverry, E. Roubaud, R. Basséguy, M.L. Délia, A. Bergel, Microbial electrolysis cell (MEC): Strengths, weaknesses and research needs from electrochemical engineering standpoint, Appl. Energy 257 (2020) 113938, https://doi.org/10.1016/j.apenergy.2019.113938.

[18] R.C. Wagner, D.F. Call, B.E. Logan, Optimal set anode potentials vary in bioelectrochemical systems, Environ. Sci. Technol. 44 (2010) 6036–6041, https://doi.org/10.1021/es101013e.

[19] L. Peng, Y. Zhang, Cytochrome OmcZ is essential for the current generation by Geobacter sulfurreducens under low electrode potential, Electrochim. Acta 228 (2017) 447–452, https://doi.org/10.1016/j.electacta.2017.01.091.

[20] K. Fricke, F. Harnisch, U. Schröder, On the use of cyclic voltammetry for the study of anodic electron transfer in microbial fuel cells, Energy Environ. Sci. 1 (2008) 144–147, https://doi.org/10.1039/b802363h.

[21] J. De Vrieze, J.B.A. Arends, K. Verbeeck, S. Gildemyn, K. Rabaey, Interfacing anaerobic digestion with (bio)electrochemical systems: Potentials and challenges, Water Res 146 (2018) 244–255, https://doi.org/10.1016/j.watres.2018.08.045.

[22] E. Yang, K.-J. Chae, M.-J. Choi, Z. He, I.S. Kim, Critical review of bioelectrochemical systems integrated with membrane-based technologies for desalination, energy self-sufficiency, and high-efficiency water and wastewater treatment, Desalination 452 (2019) 40–67, https://doi.org/10.1016/j.desal.2018.11.007.

[23] E. Roubaud, R. Lacroix, S. Da Silva, A. Bergel, R. Basséguy, B. Erable, Catalysis of the hydrogen evolution reaction by hydrogen carbonate to decrease the voltage of microbial electrolysis cell fed with domestic wastewater, Electrochim. Acta 275 (2018) 32–39, https://doi.org/10.1016/j.electacta.2018.04.135.

[24] A. Escapa, R. Mateos, E.J. Martínez, J. Blanes, Microbial electrolysis cells: An emerging technology for wastewater treatment and energy recovery. from laboratory to pilot plant and beyond, Renew. Sustain. Energy Rev. 55 (2016) 942–956, https://doi.org/10.1016/j.rser.2015.11.029.

[25] J.M. Foley, R.A. Rozendal, C.K. Hertle, P.A. Lant, K. Rabaey, Life cycle assessment of high-rate anaerobic treatment, microbial fuel cells, and microbial electrolysis cells, Environ. Sci. Technol. 44 (2010) 3629–3637, https://doi.org/10.1021/es100125h.

[26] L. De Silva Muñoz, A. Bergel, D. Féron, R. Basséguy, Hydrogen production by electrolysis of a phosphate solution on a stainless steel cathode, Int. J. Hydrog. Energy 35 (2010) 8561–8568, https://doi.org/10.1016/j.ijhydene.2010.05.101.

[27] S. Freguia, K. Rabaey, Z. Yuan, J. Keller, Electron and carbon balances in microbial fuel cells reveal temporary bacterial storage behavior during electricity generation, Environ. Sci. Technol. 41 (2007) 2915–2921, https://doi.org/10.1021/es062611i.

[28] W.E. Balch, G.E. Fox, L.J. Magrum, C.R. Woese, R.S. Wolfe, Methanogens: reevaluation of a unique biological group, Microbiol. Rev. 43 (1979) 260–296, https://doi.org/10.1128/mmbr.43.2.260-296.1979.

[29] J.G. Zeikus, The biology of methanogenic bacteria, Bacteriol. Rev. 41 (1977) 514–541, https://doi.org/10.1128/mmbr.41.2.514-541.1977.

[30] M. Zeppilli, P. Paiano, M. Villano, M. Majone, Anodic vs cathodic potentiostatic control of a methane producing microbial electrolysis cell aimed at biogas upgrading, Biochem. Eng. J. 152 (2019) 107393.

[31] G. Mancini, A. Luciano, D. Bolzonella, F. Fatone, P. Viotti, D. Fino, A water-waste-energy nexus approach to bridge the sustainability gap in landfill-based waste management regions, Renew. Sustain. Energy Rev. 137 (2021) 110441, https://doi.org/10.1016/j.rser.2020.110441.

[32] T.H.J.A. Sleutels, H.V.M. Hamelers, R.A. Rozendal, C.J.N. Buisman, Ion transport resistance in Microbial Electrolysis Cells with anion and cation exchange membranes, Int. J. Hydrog. Energy 34 (2009) 3612–3620, https://doi.org/10.1016/j.ijhydene.2009.03.004.

[33] S. Shiva Kumar, V. Himabindu, Hydrogen production by PEM water electrolysis – A review, Mater. Sci. Energy Technol. 2 (2019) 442–454, https://doi.org/10.1016/j.mset.2019.03.002.

[34] S. Slade, S.A. Campbell, T.R. Ralph, F.C. Walsh, Ionic Conductivity of an Extruded Nafion 1100 EW Series of Membranes, J. Electrochem. Soc. 149 (2002) A1556, https://doi.org/10.1149/1.1517281.

[35] Masood Ebrahimi, Chapter 13 - Fuel cell power plants, book Power Generation Technologies, Academic Press, 2023, Pages 533–574, ISBN 9780323953702, https://doi.org/10.1016/B978–0-323–95370-2.00013–2.

[36] Q. Yang, Y. Jiang, Y. Xu, Y. Qiu, Y. Chen, S. Zhu, S. Shen, Hydrogen production with polyaniline/multi-walled carbon nanotube cathode catalysts in microbial electrolysis cells, J. Chem. Technol. Biotechnol. 90 (2015) 1263–1269, https://doi.org/10.1002/jctb.4425.

[37] A. Kadier, Y. Simayi, K. Chandrasekhar, M. Ismail, M.S. Kalil, Hydrogen gas production with an electroformed Ni mesh cathode catalysts in a single-chamber microbial electrolysis cell (MEC), Int J. Hydrog. Energy 40 (2015) 14095–14103, https://doi.org/10.1016/J.IJHYDENE.2015.08.095.

[38] A.K. Chaurasia, P. Mondal, Enhancing biohydrogen production from sugar industry wastewater using Ni, Ni–Co and Ni–Co–P electrodeposits as cathodes in microbial electrolysis cells, Chemosphere 286 (2022) 131728, https://doi.org/10.1016/J.CHEMOSPHERE.2021.131728.

[39] D. Hong-Yan, Y. Hui-Min, L. Xian, S. Xiu-Li, L. Zhen-Hai, Preparation and Electrochemical Evaluation of MoS2/Graphene Quantum Dots as a Catalyst for Hydrogen Evolution in Microbial Electrolysis Cell, J. Electrochem. 27 (2021) 429–438.

[40] D. Liang, L. Zhang, W. He, C. Li, J. Liu, S. Liu, H.S. Lee, Y. Feng, Efficient hydrogen recovery with CoP-NF as cathode in microbial electrolysis cells, Appl. Energy 264 (2020) 114700, https://doi.org/10.1016/J.APENERGY.2020.114700.